Crystallinity of Polyethylene Derived from Solid-State Proton NMR Free Induction Decay

Eddy W. Hansen,[†] Per Eugen Kristiansen,*[,‡] and Bjørn Pedersen[‡]

Department of Chemistry, University of Oslo, P.O. Box 1033, Blindern, 0315 Oslo, Norway, and SINTEF Applied Chemistry, P.O. Box 124 Blindern, 0314 Oslo, Norway

Received: April 7, 1998; In Final Form: May 5, 1998

The solid-state ^{1}H NMR free induction decay (FID) signal of polyethylene (PE) has been resolved into a crystalline and an amorphous part by model fitting. The "crystalline" part of the FID is represented by the inverse Fourier transform of the "Pake" function (in the frequency domain). Likewise, the "amorphous" part of the FID is modeled as a linear combination of analytical functions of the following types: exponential (E), Gaussian (G), Weibullian (W), and Brereton (B). Model fitting and statistical evaluation of these different assemblies of functions, suggest the P-B-E model to give the best representation of the overall FID of PE. The crystallinity derived from these model fits is discussed and compared to more conventional methods of determining crystallinity, such as density measurements and differential scanning calorimetry (DSC).

Introduction

It is well-known that polyethylene crystallizes to form semicrystalline solids composed of an amorphous and a crystalline phase.[1] Also, intermediate regions, which combine these two major phases, have been reported and discussed in the literature.[2−5] A great deal of effort has been exercised to accurately determine the crystallinity of semicrystalline polymers since the relative distribution of these phases is recognized to have a significant impact on the physical properties of such polymers.[6] The most common methods have been X-ray diffraction, density measurements, and differential scanning calorimetry (DSC). Also, crystallinity derived from NMR measurements has been reported.[7−13] Application of the latter technique to determine crystallinity relies on differences in molecular mobility and/or variances in the local electronic environment of the distinct phases. These differences in molecular properties have prompted researchers in the field to apply a large variety of ^{13}C NMR techniques to ascertain crystalliny.[2,3,7−15] However, each technique has its inherent limitation. For instance, application of conventional solid-state carbon NMR suffers from extremely long spin−lattice relaxation times, T_1.[14] Depending on the applied magnetic field strength, the T_1 may extend to more than 7000 s,[16] which makes simple MAS spectroscopy rather impractical when keeping in mind that, to ensure quantitative sampling of the FID, the repetition time should be approximately 5 times the longest T_1 of the proton nuclei.

The use of different cross-polarization (CP) techniques may seemingly overcome the problem of long T_1. However, other types of relaxation processes, characterized by time constants $T_{1\rho}$ and T_{1CH}, are expected to be different in the two phases and need to be estimated before actually probing the crystallinity from such measurements.[13,17] This requirement makes also these experiments rather time-consuming. In short, ^{13}C NMR suffers from a generally much poorer signal-to-noise (S/N) ratio when compared to ^{1}H NMR.

Even if there is an important time-savings in using proton NMR, the fast decay rate (short T_2) of the crystalline part of the proton FID combined with rf-pulse breakthrough may result in a significant loss of signal intensity during the initial part of the FID. This inherent lack of observable signal intensity is caused by the need of introducing a finite blanking time of the receiver at the start of the FID (to limit rf-pulse breakthrough) with a consequent "distortion" of the Fourier transform (FT) spectrum or frequency spectrum. In particular, the derived signal intensity may be systematically erroneous. One way of resolving this difficulty is to extrapolate the observed FID back to zero time before FT is performed. Zero time is defined at the center of the rf-pulse. How to perform such an extrapolation may be rather critical and is debated thoroughly in the literature. See for instance the discussion by Engelsberg et al.[18]

If analytical functions representing the crystalline and amorphous phases were known, the quantitative analysis of crystallinity could be performed directly on the FID without having to resort to a discrete Fourier transformation. Such an approach was recently adopted by Dadayli et al.[19] in a solid-state NMR investigation of polypropylene (PP).

The object of the present work is to investigate different analytical functions that may characterize the individual FID signals originating from the crystalline and the amorphous phases of PE, respectively. The crystallinity may thus be determined by a direct model fit to the observed FID. In particular, we will look for functions that have a physical significance to the problem.

All measurements reported in this work are performed at room temperature, which is above the glass temperature and below the melting temperature of polyethylene (PE). This implies that a large difference in mobility of the strongly coupled proton pairs within the two phases is expected. This difference in mobility is known to affect the shape of the individual FIDs (crystalline/amporphous) differently.

Experimental Section

Materials. Four extruded polyethylene (PE) samples (granules), denoted PE 1−4, with varying degrees of crystallinity were received from the (Polyolefinic producer) Borealis.

* To whom correspondence should be addressed.
[†] SINTEF Applied Chemistry.
[‡] University of Oslo.

S1089-5647(98)01753-2 CCC: $15.00
Published on Web 06/18/1998

Samples PE 1 and PE 2 are low-density PE samples, while samples PE 3 and PE 4 are medium- and high-density polyethylenes, respectively. The crystallinities were derived from density and differential scanning calorimetry (DSC) measurements. Measured crystallinities ranged from 45% to 72%. The samples were analyzed by solid-state ^{1}H NMR without further treatment.

NMR. All NMR measurements were performed on a Bruker DMX 200 AVANCE instrument operating at 200 MHz proton resonance frequency. A high-power ^{1}H NMR probe capable of producing 90° radio frequency (rf) pulses of approximately 1.3 μs was used. The FID was sampled every 0.2 μs. Due to pulse breakthrough, a receiver blanking time ("dead time") of 2 μs was applied. Sixty four scans were acquired in each experiment, with a repetition time of 20 s between each scan. This repetition time is much longer than 5 times the longer spin−lattice relaxation time T_1 (<1.5 s) of the methylene protons and ensures quantitative sampling of the FID. To assure that only the real part of the FID is sampled, the actual phase parameters were adjusted manually to give a pure absorption spectrum.[20] The real part of the FID was transferred to an external PC for post processing. Approximately 400 points of the FID (the first 200 points and then every fourth point of the residual part of the FID) were subjected to a nonlinear least-squares fit, using a simplex algorithm. All measurements were performed at room temperature, i.e., 298 K.

Theoretical Outline

Crystalline Phase. From a NMR point of view, PE represents a rather "simple" polymer system in which the two proton nuclei of each methylene group constitute a strong dipole−dipole-coupled two-spin system. Due to the weaker dipole−dipole coupling between protons on different methylene groups, the absorption line shape function of the protons in PE can be considered, to a good approximation, to arise from a Gaussian-broadened two-spin interaction, where the broadening is due to the other neighbors. Pake[21] has deduced an analytical expression for such an absorption spectrum of coupled spin $^1/_2$ nuclei (see Results and Discussion section). However, due to the inherent NMR dilemma related to rf-pulse breakthrough, as pointed out in the Introduction section, the theoretical Pake function cannot be fitted directly to the frequency spectrum. We need to obtain the inverse Fourier transform of the Pake expression, which will represent the observed signal intensity in the time domain. This is not a trivial issue to work out. However, Look and co-workers[22] presented an analytical solution to this enigma;

$$P(t) = \sqrt{\frac{\pi}{6}}\exp\left[-\frac{1}{2}\beta^2 t^2\right]\left\{\frac{\cos \alpha t}{\sqrt{\alpha t}}C\left[\sqrt{\frac{6\alpha t}{\pi}}\right] + \frac{\sin \alpha t}{\sqrt{\alpha t}}S\left[\sqrt{\frac{6\alpha t}{\pi}}\right]\right\} \quad (1a)$$

where $P(t)$ defines the normalized time-dependent FID signal and $C[x]$ and $S[x]$ are the so-called Fresnell functions which are defined as integral equations.[23] The parameter α is related to the distance, R_{H-H}, between the two nearest neighbor protons of the methylene group:

$$\alpha = \frac{3\gamma^2\hbar}{4R_{H-H}^3} \quad (1b)$$

where γ is the nuclear gyromagnetic ratio and $\hbar$ is Planck's constant. β represents the width of the Gaussian broadening function, which takes account of dipole−dipole interactions between protons on different methylene groups. To apply eq 1a as a fitting function, a more tractable form of the Fresnell functions is needed. We have used the following approximations:[23]

$$C(x) = \frac{1}{2} + f(x)\sin\left[\frac{\pi}{2}x^2\right] - g(x)\cos\left[\frac{\pi}{2}x^2\right] \quad (1c)$$

$$S(x) = \frac{1}{2} - f(x)\cos\left[\frac{\pi}{2}x^2\right] - g(x)\sin\left[\frac{\pi}{2}x^2\right] \quad (1d)$$

where

$$f(x) = \frac{1 + 0.926x}{2 + 1.792x + 3.104x^2} + \epsilon(x) \quad (1e)$$

$$g(x) = \frac{1}{2 + 4.142x + 3.492x^2 + 6.670x^3} + \epsilon(x) \quad (1f)$$

The absolute error, $\epsilon(x)$, in these approximations is less than 2×10^{-3}.

Dadayli et al.[19] have used an approximate form of eq 1a, which is defined by a Gaussian-broadened sinc function, defined by

$$A(t) = \frac{\sin(2\pi\nu t)}{2\pi\nu t}\exp\left(-\left(\frac{t}{T_2^*}\right)^2\right) \quad (2)$$

This function was first suggested by Abragam[24] as a phenomenological expression of the ^{19}F FID of CaF_2 and is, in this work, simply denoted an "Abragamian". This expression has been found to be a good representation for the FID from other regular, crystalline lattices.[19]

Amorphous Phase. In contrast to the crystalline phase of PE, the amorphous phase is characterized by an increased fluctuation in the molecular mobility, which is expected to modify the shape of the NMR spectrum. Brereton et al.[25] have derived an exact, theoretical expression for the FID of a dynamic scale invariant polymer chain governed by a single relaxation time. This type of function has been shown to give a satisfactory representation of the FID of amorphous PE above its glass transition temperature, T_g. This same function has been shown to give a reasonable reproduction of the FID from PE melts over a range of temperatures. The analytical form of the "Brereton" function, $B(\Delta,\tau,t)$, is given below:[25]

$$B(\Delta,\tau,t) = |g(2\Delta,t)||g(-\Delta,t)|^2\cos[\varphi(2\Delta,t) + 2\varphi(-\Delta,t)] \quad (3)$$

where

$$|g| = \left[\frac{a^2 + b^2}{A^2 + B^2}\right]^{1/4}\exp\left[-(a-1)\frac{t}{2\tau}\right] \quad (3a)$$

and

$$\varphi = \frac{1}{2}\left[\tan^{-1}\frac{b}{a} - \tan^{-1}\frac{B}{A}\right] - b\frac{t}{2\tau} \quad (3b)$$

The parameters a, b, A, and B are expressed by the following equations:

$$a = [1 + (2\Delta\tau)^2]^{1/4} \cos\left[\frac{1}{2}\tan^{-1}(2\Delta\tau)\right] \quad (3c)$$

$$b = [1 + (2\Delta\tau)^2]^{1/4} \sin\left[\frac{1}{2}\tan^{-1}(2\Delta\tau)\right] \quad (3d)$$

$$A = (1 + a)^2 - b^2 - \left[\{(1 - a)^2 - b^2\} \cos\frac{2tb}{\tau} - 2b(1 - a) \sin\frac{2tb}{\tau}\right] \exp\left[-\frac{2ta}{\tau}\right] \quad (3e)$$

$$B = 2b(1 + a) + \left[2b(1 - a) \cos\frac{2tb}{\tau} + 2\{(1 - a)^2 - b^2\} \sin\frac{2tb}{\tau}\right] \exp\left[-\frac{2ta}{\tau}\right] \quad (3f)$$

The parameter Δ is related to the α factor (eq 1b) in the Pake function according to

$$\Delta = \frac{2\alpha}{N_a} \quad (3g)$$

in which N_a represents a small number of ethylene monomer units forming a segment of PE. Thus, Δ defines a rescaled dipole interaction strength, which determines the basic inverse time scale of the model.[24,25] Dadayli et al.[19] have pointed out that the rather complex "Brereton" function can be well approximated by the sum of a Weibullian function and one or two exponential functions. The normalized Weibullian function is defined by eq 4:

$$W(t) = \exp\left[-\left(\frac{t}{T_c}\right)^n\right] \quad (4)$$

and ranges between a pure Lorentzian ($n = 1$) and a pure Gaussian ($n = 2$). It should be emphasized, however, that there is no direct theoretical justification for the approximation of a "Brereton" function to a sum of a Weibullian and one or two exponential functions. This approximation is basically an empirical one. Although the analytical expression of the "Brereton" function is fairly elaborate, its main advantage relies on the few parameters (Δ and τ) needed to describe this function. This is in contrast to its corresponding approximate expression—represented by a Weibullian and one or two exponentials—which needs four and six parameters, respectively, to be uniquely defined.

Results and Discussion

Differential Scanning Calorimety (DSC) and Density Measurements. The density (ρ) and heat of melting, ΔH (from DSC), of the polyethylene samples reported in this work are shown in Table 1. The fraction crystallinity, λ (%), is calculated from eqs 5a[9] and 5b,[27] respectively:

$$\lambda_{DSC} = 100\frac{\Delta H}{\Delta H^*} \quad (5a)$$

$$\lambda_\rho = 100\frac{1/\rho_a - 1/\rho}{1/\rho_a - 1/\rho_c} \quad (5b)$$

where ΔH is the heat of melting of 1 mg of polyethylene and ΔH^* (=286 J) is the heat of melting of 1 mg of a single crystal of PE.[28] The densities of completely amorphous and crystalline PE are denoted ρ_a (=0.852 g·cm^{-3}) and ρ_c (=1.000 g·cm^{-3}), respectively.[29]

TABLE 1: Melting Temperature (T_{melt}), Melting Enthalpy (ΔH_{melt}), Density (ρ), and Derived Crystallinity of the Four PE Samples Investigated

	PE 1	PE 2	PE 3	PE 4
T_{melt} (°C)	111.7	123.4	127.1	131.6
ΔH_{melt} (J/mg)	134.9	129.9	178.3	208.7
ρ (g/cm^3)	0.922	0.919	0.935	0.943
crystallinity; λ_{DSC} (eq 5a)	46.5	44.8	61.5	72.0
crystallinity; λ_ρ (eq 5b)	51.3	49.3	59.3	65.2

Under the assumption that no interfacial region exists, the crystallinity fractions derived from eqs 5a and 5b are expected to be identical. The observed difference in crystallinity derived from density and DSC measurements (Table 1) may be explained by the existence of an interfacial region of density ρ_I. Denoting the mass fraction of the intermediate phase within the noncrystalline region by α, the following equation can easily be derived:

$$\rho_I = \frac{\alpha\rho_C(1 - \lambda_{DSC})}{(\lambda_\rho - \lambda_{DSC})(1 - \rho_C/\rho_A) + \alpha(1 - \lambda_{DSC})\rho_C/\rho_A} \quad (5c)$$

where all symbols have been defined previously. Figure 1 shows how the density of the intermediate phase will depend on the mass fraction α of samples PE 1 and PE 2, according to eq 5c. From these calculations it is not possible to uniquely characterize the intermediate phase. Only the lower limit of α can be estimated and is seen to be larger than 7 wt %. The density of the intermediate phase may take any value between 0.852 (amorphous) and 1 (crystalline). However, when the crystallinity derived from DSC is larger than the corresponding crystallinity derived from density measurement (samples PE 3 and PE 4; Table 1), eq 5c is no longer valid.

The difference in crystallinity obtained from DSC and density measurements may originate from uncertainties in the densities ρ_C and ρ_A of eq 5b. Also, the density of the crystalline phase may depend on the polymer characteristics, i.e., whether the sample is a low-density, a medium-density, or a high-density polyethylene. However, this subject is outside the scope of this work and will not be discussed further.

Before discussing how to obtain crystallinity from the FID, a conventional analysis of the NMR frequency spectrum will be considered in lieu of the inherent and inevitable application of a receiver dead time.

Spectral Analysis. Figure 2A shows a series of FT ^{1}H NMR spectra of sample PE 4 for different prefixed values of the receiver dead time. Use of a receiver dead time larger than 4 μs was found to be essential in order to minimize the effect of rf-pulse breakthrough. Fitting the sum of a Pake function (eq 6a), which represents the crystalline phase, and two Lorentzian

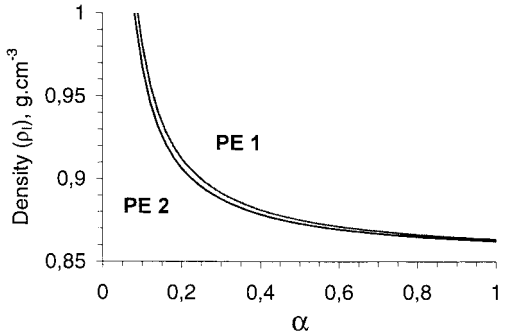

Figure 1. Relation between density (ρ_I) and mass-fraction (α) of the intermediate phase of the noncrystalline region of samples PE 1, PE 2. See text for further details.

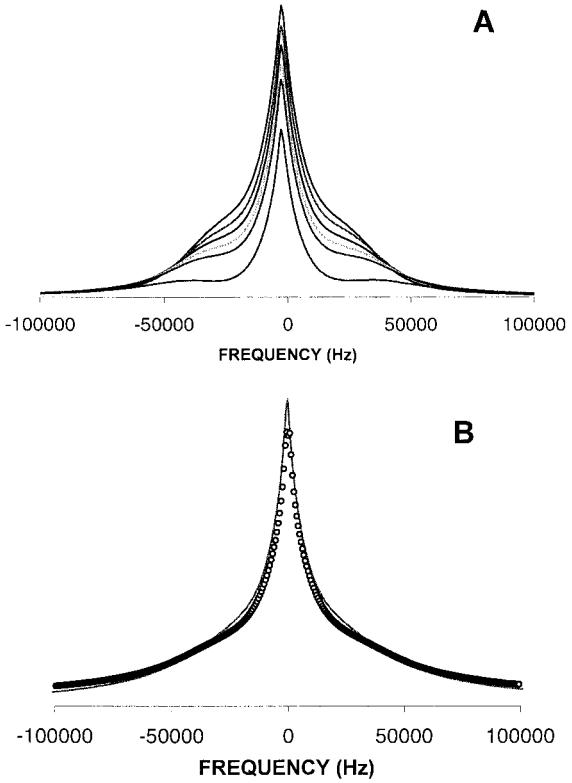

Figure 2. (A) FT ^{1}H NMR spectra vs receiver dead time of sample PE 4. The dead times are—from bottom to top—equal to 4, 5, 6, 7, 8, and 12 μs, respectively. (B) Nonlinear least-squares fit of a sum of a Pake function and two exponential functions (solid curve) to the observed FT spectrum (open circles) of sample PE 4 (dead time = 5 μs).

functions (amorphous phase) to the observed spectra in Figure 2A enables the apparent crystallinity to be derived. An illustration of such a model fit is shown in Figure 2B. The apparent crystallinity is determined from the intensity ratio of the Pake function (F_0) and the total intensity of the spectrum. In this work, the term "Pake" is attributed to both the frequency function (eq 6) and the time function or FID (eq 1) of the crystalline phase. No distinction is made, since the two functions constitute a Fourier transform pair.

$$F(\omega) = \int_{-\infty}^{+\infty} \rho(x)\, g(\omega - x)\, \mathrm{d}x \tag{6a}$$

where

$$\rho(x) = \rho_+(x) + \rho_-(x) \tag{6b}$$

$$\rho_+(x) = F_0 \frac{1}{\sqrt{1 + x/\alpha}}; \quad -\alpha < x < 2\alpha \tag{6c}$$

$$\rho_+(x) = 0; \quad \text{otherwise} \tag{6d}$$

$$\rho_-(x) = F_0 \frac{1}{\sqrt{1 - x/\alpha}}; \quad -2\alpha < x < \alpha \tag{6e}$$

$$\pi_+(x) = 0; \quad \text{otherwise} \tag{6f}$$

and

$$g(u) = \frac{1}{\sqrt{2\pi\beta^2}} \exp\left[-\frac{u^2}{2\beta^2}\right] \tag{6g}$$

The parameters α and β are defined in eq 1. The apparent crystallinity derived from this spectral deconvolution is plotted as a function of dead time (Figure 3) and shows a decrease with increasing dead time. Due to the absence of any theoretical model that relates the apparent crystallinity to dead time, a simple second-order polynomial function is used to fit the observed data. This fit enables the apparent crystallinity to be estimated and equals 68.6 ± 3.0% (at zero dead time).

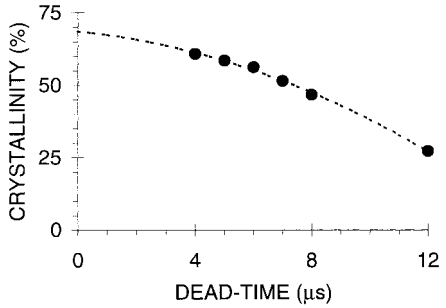

Figure 3. Apparent "crystallinity" vs instrumental dead time as derived from the FT ^{1}H NMR spectra of Figure 2.

TABLE 2: Combination of Analytical Functions Used to Fit the Observed FIDs

analytical function[a]	correlation coefficient (r)	Z-value[b]
PB	0.997 746	3.39
PE2	0.998 94	3.77
PWE	0.999 931	5.14
PGE	0.999 884	4.88
PBE	0.999 988	5.99
PE	0.994 572	2.95
AWE2	0.999 900	4.95

[a] The following short-hand notation is used: P ("Pake"), E ("exponential"), W ("Weibullian"), G ("Gaussian"), B ("Brereton"), A ("Abragamian"). [b] See text for further details.

FID Analysis: Method of Approach. The type of analytical functions (model) that are chosen to represent the observed FID decay are summarized in Table 2. For simplicity, a three-letter notation XYZ is used, which represents a sum of the three functions X, Y, and Z. The three functions are selected from the following group of "analytical" functions: P (Pake), W (Weibullian), G (Gaussian), L(Lorenzian), B ("Brereton"), and A (Abragamian). The mathematical expression of these functions has been defined in a previous section.

Initially, each model (see Table 2) was fitted to the observed FID of samples PE 1−4 without any constraint. Figure 4 illustrates one such fit to the PBE model. The value of the α parameter of the Pake function derived from this fit was found to be 1.194×10^5 s^{-1} (PE 1), 1.205×10^5 s^{-1} (PE 2), 1.001×10^5 s^{-1} (PE 3), and 1.444×10^5 s^{-1} (PE 4), respectively. The resulting error distribution, i.e., the difference between the PBE model fit and the observed FID of sample PE 2, is illustrated in Figure 5A and suggests that the residuals are nearly randomly distributed. The slight oscillatory behavior of the residual versus time (Figure 5A) may suggest that additional components of the model FID are needed to completely describe the observed FID. Adding a fourth component (E) to the model FID (PBE_2 model) did, however, not improve the subsequent fit. This kind of small oscillatory behavior of the residual versus initial time was observed in most of the applied models. The amplitude of the oscillation was generally so small that we chose to disregard it.

As pointed out by Dadayli et al.,[19] a simple way to increase the effective signal-to-noise ratio, and to constrain the fitting more effectively, is to perform a fit to all the FIDs simulta-

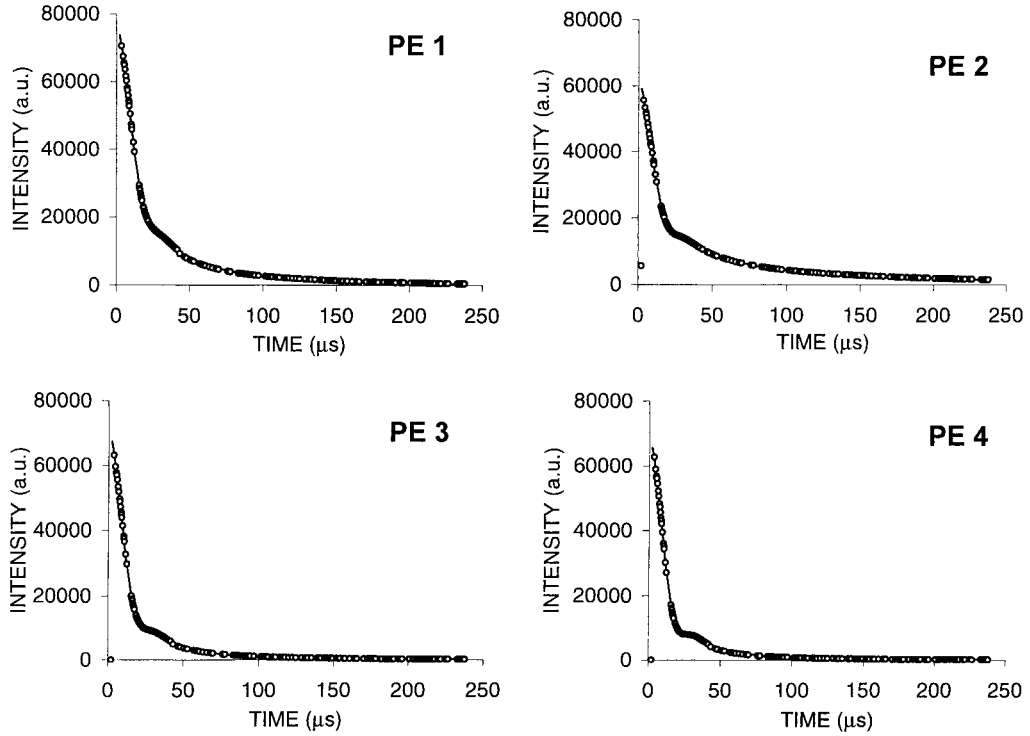

Figure 4. Observed FIDs (○) and corresponding best fits (solid curves) to a PBE model of samples PE 1, PE 2, PE 3, and PE 4.

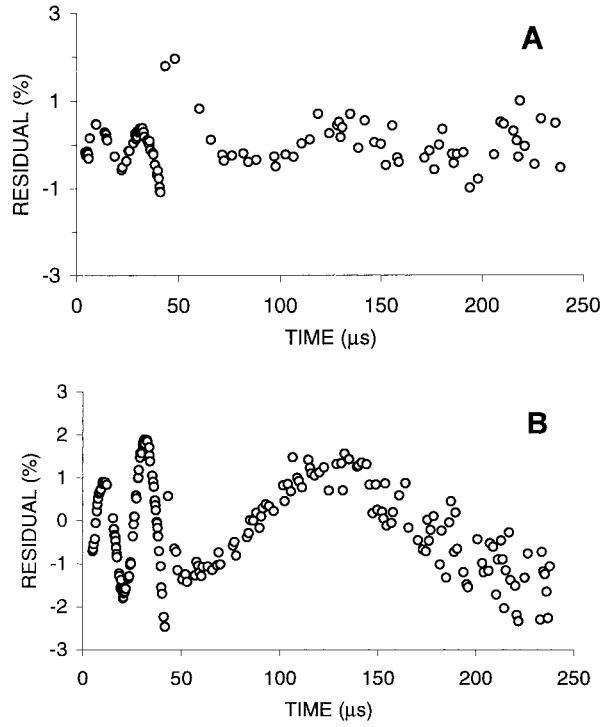

Figure 5. (A) Error distribution between model FID (PBE model) and observed FID of sample E 1 with no constraint. (B) Corresponding error distribution curve derived from a constrained model fit. See text for further details.

neously. Since, to our knowledge, there is no obvious reason to expect the shape of the Pake function to be different from one sample to another, we decided to perform a simultaneous fit to all the samples under the constraint that the parameters α and β of the Pake function were identical; that is, α(PE 1) = α(PE 2) = α(PE 3) = α(PE 4) and β(PE 1) = β(PE 2) = β(PE 3) = β(PE 4). As can be inferred from Figure 5B, the oscillatory behavior of the residual versus time becomes somewhat more distinct. However, the amplitude of the oscillation is still small.

Of particular importance, the proton−proton distance (R_{H-H}) within a methylene group can be calculated from eq 1b, resulting in $R_{H-H} = 1.684$ Å. From simple geometric consideration, the corresponding C−H distance can be written $R_{C-H} = R_{H-H}/\sin(\theta/2)$, where θ is the H−C−H bond angle. From X-ray measurements at room temperature,[30−32] θ was found to be 107°. Inserting this latter parameter into the above equation gives $R_{C-H} = 1.048$ Å, which is in excellent agreement with the value of 1.069 Å, as determined by X-ray measurements.[30−32] These results encouraged us to use the "simultaneous fitting approach" to all models studied in this work.

Statistical Evaluation.[33] To decide which model (Y_{calc}) gives the better fit to a set of experimental data (Y_{obs}), we will compare their coefficient of correlations, r, as defined by

$$r = \frac{\sum_i (Y_{i,\mathrm{calc}} - \bar{Y})^2}{\sum_i (Y_{i,\mathrm{obs}} - \bar{Y})^2} \tag{7a}$$

where

$$\bar{Y} = \frac{\sum_i Y_{i,\mathrm{obs}}}{N} \tag{7b}$$

N is the number of data points, and $\bar{Y}$ is the average of $Y_{i,obs}$. To decide whether a significant difference between two models exists, the so-called Fisher's Z-transform will be applied:

$$Z = \frac{1}{2}\ln\left[\frac{1+r}{1-r}\right] \tag{7c}$$

The following parameter is also needed:

$$\sigma_{Z_1 - Z_2} = \sqrt{\frac{1}{N - N_{p1}} + \frac{1}{N - N_{p2}}} \tag{7d}$$

where N_{pi} represents the number of adjustable parameters of model i.

TABLE 3: Apparent Crystallinites Obtained by Constrained Model Fits to the Observed FIDs of Samples PE 1−4. See Text for Further Details

model[a]	crystallinity PE 1	PE 2	PE 3	PE 4
PB	60	65	73	79
PE_2	43	51	61	69
PWE	58	64	76	86
PGE	58	61	72	78
PBE (no constraints)	40	53	60	67
PBE	49	50	59	68
PE	57	64	70	77
AWE_2	36	40	51	58

[a] The following short-hand notation is used; P ("Pake"), E ("exponential"), W ("Weibullian"), G ("Gaussian"), B ("Brereton"), A ("Abragamian").

We then use the fact that the test statistic

$$z = \frac{Z_1 - Z_2}{\sigma_{Z_1 - Z_2}} \tag{7e}$$

is normally distributed. Since, N ($\approx$440) $\ll N_{pi}$ ($\leq$10), eq 7e can be simplified to give $z = (Z_1 - Z_2)/\sqrt{2/N}$. If $z > z_{tab} = 1.96$ (95% confidence interval), the model with the larger r value represents a statistically better model.

The underlying assumption that z is normally distributed may be questionable. Since too few data sets are available in this work, we are not able to take this assumption as a fact, which may lead to some ambiguity regarding the result of the significance test. However, in most cases, the statistical validity test can be qualitatively confirmed by visual inspection of the observed error curves.

Crystallinity. The apparent crystallinity reported in this work is simply estimated from the intensity ratio of the Pake/Abragamian function, divided by the total signal intensity of the FID at zero time.

The calculated Z value of the different models is presented in Table 2 and suggests the PBE model to represent the best fit to the observed data. The crystallinities obtained by the constraint model fit (PBE model) are 49% (PE 1), 50% (PE 2), 59% (PE 3), and 68% (PE 4), respectively. Except for sample E 1, these crystallinities are—within experimental error—the same as obtained by the nonconstraint model fit (Table 3) of 53% (PE 2), 60% (PE 3), and 67% (PE 4), respectively.

The significant difference in crystallinity derived for sample E 1 of 40% (nonconstraints) and 49% (constraint), respectively, is not understood. Of particular importance, however, is the excellent agreement in crystallinity obtained by the constraint PBE model fit (Table 3) and density/DSC measurements (Table 1). From the statistical analysis, the PB, PL, and PE_2 models give rather poor fits to the observed FIDs. The remaining models, PWE, PGE, and AWE_2, provide significantly better fits. However, they do not give as good a fit as the PBE model.

The apparent crystallinities derived from the different models are summarized in Table 3 and demonstrate that the PBE model gives the best estimate of crystallinity, when compared to density and DSC measurements.

Note also the strikingly good agreement in apparent crystallinity obtained from the FID analysis (68%; Table 3) and from the "extrapolated" frequency spectrum (68.6%; Figure 3) of sample PE 4.

Noncrystalline Phases. Figure 6a shows the three resolved functions *P*, *B*, and *E* of the PBE model fit to the FID of sample PE 1. The oscillatory character of the crystalline part of the FID (Pake function) is frequently encountered from crystals without pronounced motional narrowing. Note in particular the fast initial decay of this function, which is reduced by approximately 25% during the first 6 μs. A more tractable representation of the three functions is given in Figure 6B, which shows the FT spectra of the three functions. In particular, the doublet structure of the Pake function can be revealed. This doublet structure becomes less pronounced with increasing β/α ratio. When this ratio becomes larger than 0.70, the spectrum will show no fine structure and equals the spectrum of a uniform distribution of atomic nuclei.[34] In this work, β was found to be equal to 0.695×10^5 s^{-1}, which results in $\beta/\alpha = 0.58$. Thus, the observed "splitting" of the Pake function is rather modest.

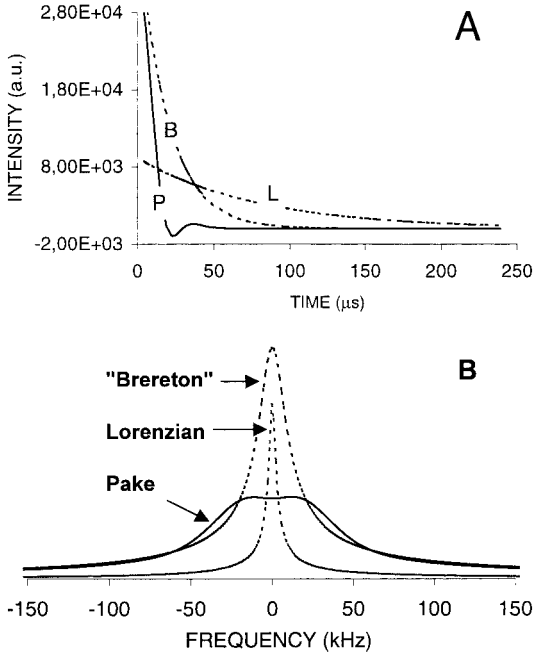

Figure 6. (A) Illustration of the P ("Pake"), B ("Brereton"), and E ("Exponential") functions as derived from a nonlinear least-squares fit of a BPE model fit (with constraints) to the observed FID of sample PE 1. See text for further details. (B) Corresponding FT spectra of the three functions.

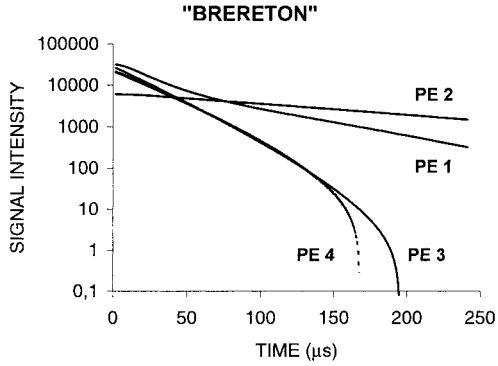

Figure 7. Illustration of the "Brereton" functions as derived from a nonlinear least-squares fit of a BPE model fit (with constraints) to the observed FID of samples PE 1−4. See text for further details.

Except for sample PE 2, the decay of the "Brereton" functions is seen to deviate from a purely exponential decay (Figure 7). Brereton[25] has discussed this phenomenon in detail and found that an exponential decay is expected when the product between the parameters Δ and τ is significantly less than 1. For the samples investigated in this work, these products were found to be 14.8 (PE 1), 0.63 (PE 2), 0.28 (PE 3), and 0.78 (PE 4). For times $t < 100$ μs, the "Brereton" functions of samples PE

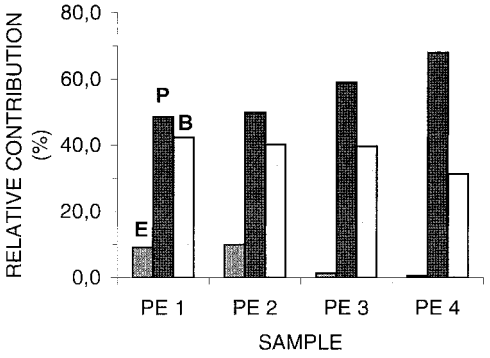

Figure 8. Relative intensity contribution (in percent) of the functions P ("Pake"), B ("Brereton") and E ("Exponential") as derived from a nonlinear least-squares fit of a BPE model fit (with constraints) to the observed FID of sample PE 1−4. See text for further details.

3 and PE 4 can be approximated by single-exponential functions with spin−spin relaxation times, T_2, of 25 and 27.4 μs, respectively. In contrast, the "Brereton" function of the PE 2 sample, which can be represented by a single-exponential function in the whole experimental time domain, reveals a T_2 of 169 μs. This indicate that the molecular motional characteristics within sample PE 2 and samples PE 3/PE 4 are different. Referring to the basic work of Brereton et al.,[25,26] additional detailing of these motional characteristics may be accomplished. However, this area is outside the scope of this work.

The relative contribution from the different functions of the PBE model is displayed in Figure 8 for all four samples. The signal intensity from the purely exponential part decreases from approximately 10% in sample PE 1 to less than 1% in sample PE 4. Likewise, a corresponding decrease in the intensity of the "Brereton" function can be seen, which decreases from approximately 42% in sample PE 1 to approximately 31% in sample PE 4. Since the "Brereton" function of sample PE 2 is equivalent to a purely "exponential" function, we have simply assigned the larger peak intensity of the two "exponential" functions to the "Brereton" intensity. It is tempting to assign the exponential part of the FID to a purely amorphous phase and the corresponding "Brereton" function to a mixed, intermediate phase. However, it may be that the two functions, "Brereton" and "Exponential", which are needed to characterize the amorphous phase, are intimately connected and are not "physically" separable. Whatever reason, this subtle and intriguing subject needs further investigation.

Conclusion

Different mathematical/physical models have been assembled to describe the FID obtained from PE at room temperature. Using statistical methods, a model composed of a linear combination of a "Pake" function, a "Brereton" function, and an "exponential" function is shown to give the best fit to the observed FID. The "Pake" function is ascribed to the crystalline phase, while the other two functions are ascribed to the amorphous/intermediate phases. The NMR-derived crystallinities are in good agreement with corresponding crystallinities obtained from density and DSC measurements.

Acknowledgment. We are grateful to Borealis AS for performing the DSC measurements and for making the samples available for NMR characterization. We also thank Dr. Keith Redford for making corrections to the text.

References and Notes

(1) Bassett, D. C. *Principles of Polymer Morphology*; Cambridge University Press: Cambridge, 1981.
(2) Kitamaru, R.; Horri, F. *Adv. Polym. Sci*. **1978**, *26*, 137−178.
(3) Bergman, K. *J. Polym. Sci.*: *Polym. Phys. Ed.* **1978**, *26*, 1611−1634.
(4) Kitamaru, R.; Horri, F.; Murayama, K. *Macromolecule* **1986**, *19*, 636−643.
(5) Chen, J.; Fone, M.; Redy, V. N.; Schwartz, K. B.; Fisher, K. B.; Wunderlich, B. *J. Polym. Sci: Part B: Polym. Phys.* **1994**, *32*, 2683−2693.
(6) Boyd, R. H. *Polym. Rev.* **1985**, *26*, 323−447.
(7) Hughes, C. D.; Sethi, N. K.; Baltisberger, J. H.; Grant, D. M. *Macromolecules* **1989**, *22*, 2551−2554.
(8) Craig, D.; Doskočilová, D.; Schneider, B.; Jakeš, J.; Schmidt, P.; Baldrian, J.; Hernández-Fuentes, I.; Alonso, M. C. *Polymer* **1986**, *27*, 1658−1664.
(9) Kitamaru, R.; Horii, F.; Hyon, S.-H. *J. Polym. Sci.: Polym. Phys. Ed*. **1977**, *15*, 821−836.
(10) Nakagawa, M.; Horii, F.; Kitamaru, R. *Polymer* **1990**, *31*, 323−328.
(11) Natansohn, A. *Chem. Mater.* **1992**, *4*, 182−187.
(12) Russel, K. E.; MCFaddin, D. C.; Hunter, B. K.; Heyding, R. D. *J. Polym. Sci.: Part B: Polym. Phys.* **1996**, *34*, 247−2458.
(13) Packer, K. J.; Poplett, I. J. F.; Taylor, M. J.; Vickers, M. E.; Whiiaker, A. K.; Williams, K. P. J. *Makromol. Chem., Macromol. Symp.* **1990**, *34*, 161−170.
(14) Axelson, D. E.; Mandelkern, L.; Popli, R.; Mathieu, P. *J. Polym. Sci., Part B* **1983**, *21*, 2319−2335.
(15) Ueda, T.; Takeda, S.; Nakamura, N.; Chihara, H. *Bull. Chem. Soc. Jpn.* **1991**, *64*, 1299−1304.
(16) Kitamaru, R.; Horii, F.; Zhu, Q.; Basset, D. C.; Olley, R. H. *Polymer* **1994**, *35*, 1171−1181.
(17) Perez, E.; VanderHart, D. L. *J. Polym. Sci.*: *Part B, Polym. Phys.* **1988**, *26*, 1979−1993.
(18) Engelsberg, M.; Lowe, I. J. *Phys. Rev.* **1974**, *10*, 822−832.
(19) Dadayli, D.; Harris, R. K.; Kenwright, A. M.; Say, B. J.; Sünnetçioğlu, M. M. *Polymer* **1994**, *35*, 4083−4088.
(20) Private communication, Hans Förster (BRUKER).
(21) Pake, G. E. *J. Chem. Phys.* **1948**, *16*, 327.
(22) Look, D. C.; Lowe, I. J.; Northby, J. A. *J. Chem. Phys.* **1966**, *44*, 3441−3452.
(23) Abramowitz; Stegun, I. *Handbook of Mathematical Functions*; Dover Publ., Inc.: New York, 1970; pp 300−303.
(24) Abragam, A. *Principles of Nuclear Magetism*; Oxford University Press: Oxford, 1961; p 120.
(25) Brereton, M. G. *J. Chem. Phys*. **1991**, *94*, 2136−2142.
(26) Brereton, M. G.; Arden, I. M.; Boden, N.; Wright, P. *Macromolecules* **1991**, *24*, 2068−2074.
(27) Zimmerman, O. E.; Cui, C.; Wang, X.; Atvars, T. D. Z.; Weiss, R. G. *Polymer* **1998**, *39*, 1177−1185.
(28) Gray, A. P. *Thermochim. Acta* **1970**, *1*, 563.
(29) Elias, H. G. In *Macromolecues*; Plenum: New York, 1977; Vol. 1, pp 163−164.
(30) Bunn, C. W. *Trans. Faraday Soc.* **1939**, *35*, 482.
(31) Shearer, H. M. M.; Teare, P. W. *Acta Crystallogr*. **1956**, *12*, 294.
(32) Kavesh, S.; Schultz, J. M. *J. Polym. Sci.; Part A-2* **1970**, *8*, 243.
(33) Spiege, M. R. *Theory and Problems of Statistics*; Schaum's Outline Series; McGraw-Hill Book Co.: New York, 1972,
(34) Pedersen, B. *Acta Chem. Scand.* **1968**, *22*, 444−452.